Ionization and pulse lethargy effects in inverse Cherenkov accelerators

P. Sprangle,[1] B. Hafizi,[2] and R. F. Hubbard[1]

[1]*Beam Physics Branch, Plasma Physics Division, Naval Research Laboratory, Washington, D.C. 20375*
[2]*Icarus Research, Inc., P.O. Box 30780, Bethesda, Maryland 20824-0780*

Ionization processes limit the accelerating gradient and place an upper limit on the pulse duration of the electromagnetic driver in the inverse Cherenkov accelerator (ICA). Group velocity slippage, i.e., pulse lethargy, on the other hand, imposes a lower limit on the pulse duration. These limits are obtained for two ICA configurations in which the electromagnetic driver (e.g., laser or millimeter wave source) is propagated in a waveguide that is (i) lined with a dielectric material or (ii) filled with a neutral gas. In either configuration the electromagnetic driving field is guided and has an axial electric field with phase velocity equal to the speed of light in vacuum, c. The intensity of the driver in the ICA, and therefore the acceleration gradient, is limited by tunneling and collisional ionization effects. Partial ionization of the dielectric liner or gas can lead to significant modification of the dispersive properties of the waveguide, altering the phase velocity of the accelerating field and causing particle slippage, thus disrupting the acceleration process. An additional limitation on the pulse duration is imposed since the group velocity of the driving pulse is less than c and the pulse slips behind the accelerated electrons. Hence for sufficiently short pulses the electrons outrun the pulse, terminating the acceleration. Limitations on the driver pulse duration and accelerating gradient, due to ionization and pulse lethargy, are estimated for the two ICA configurations. Maximum accelerating gradients and pulse durations are presented for a 10 μm, 1 mm, and 1 cm wavelength electromagnetic driver. The combination of ionization and pulse lethargy effects impose severe limitations on the maximum energy gain in inverse Cherenkov accelerators. [S1063-651X(97)11505-7]

PACS number(s): 41.75.Lx

I. INTRODUCTION

Although high power sources of electromagnetic radiation, such as lasers, are capable of providing extraordinarily high electric fields for the acceleration of particles, numerous fundamental and technological issues must be resolved before practical high gradient accelerators can be realized [1–11]. There are three fundamental issues that must be addressed in any type of high gradient accelerator. These are (i) radiation beam guiding over extended distances, (ii) phase coherence (phase velocity slippage) between the accelerated particles and the electromagnetic field, and (iii) material ionization arising from either the driver fields or from the accelerated particles.

In this paper we analyze and discuss the fundamental issues as they relate to the inverse Cherenkov accelerator (ICA) [12–18]. The electromagnetic driver in the ICA can be an intense laser or millimeter wave pulse. In free space and in the absence of boundaries the phase velocity of the accelerating field exceeds the vacuum speed of light, c. As a consequence, particles continually phase slip relative to the field, i.e., phase velocity slippage and, after a slippage distance, acceleration ceases. In the ICA the phase velocity of the accelerating field is reduced by introducing a gas in the accelerating region or by lining the interior of a waveguide with a dielectric material.

A dielectrically lined or gas-filled waveguide ICA configuration (i) avoids diffraction of the driving electromagnetic beam, (ii) overcomes electron slippage, and (iii) the acceleration in the dielectrically lined ICA is in a vacuum. However, the large electric fields associated with short, intense electromagnetic pulses can readily ionize the dielectric material or gas [5,19–22]. Partial volume ionization will modify the dispersive characteristics of the waveguide, due to plasma formation. A small amount of ionization can result in the disruption of the acceleration process since the phase velocity of the electromagnetic fields will be altered, resulting in phase velocity slippage. Ionization effects therefore impose an upper limit on the pulse duration. However, the driving pulse cannot be arbitrarily short since the pulse, having a group velocity less than c, can slip behind the accelerated electrons. This effect is referred to as group velocity slippage or pulse lethargy and places a lower limit on the pulse duration. The combination of ionization and pulse lethargy effects imposes severe limitations on the energy gain in inverse Cherenkov accelerators. For sufficiently high current densities, the self-fields of the accelerated electron beam may also result in ionization. Self-field ionization processes will not be considered in this paper.

This paper is organized as follows. In Sec. II we derive and discuss various limits of the dispersion relation for transverse-magnetic (TM) modes of a dielectrically lined optical waveguide. This TM mode consists of a radial and an axial electric field as well as an azimuthal magnetic field. The axial electric field, which is responsible for acceleration, is peaked on axis, while the radial electric field vanishes on axis. In Sec. III we derive the critical average plasma density. When the average plasma density reaches this critical value the dispersive properties are modified and the phase velocity of the electromagnetic wave is significantly altered, resulting in phase velocity slippage. In Sec. IV the buildup of plasma density within the dielectric material is analyzed. Here we assume that ionization takes place within the dielectric, i.e., surface effects are neglected. This analysis is based
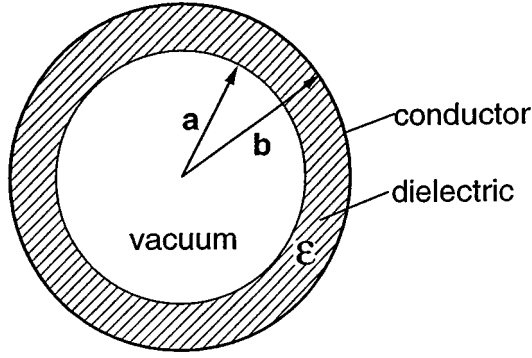
FIG. 1. Schematic of a dielectrically lined optical waveguide. The dielectric material with dielectric constant ε lies between the vacuum ($0 \leq r \leq a$) region and perfect conductor at $r = b$.

on a rate equation for plasma generation, which includes tunneling and collisional (avalanche) ionization. In Sec. V we obtain an expression for the limit on the electromagnetic pulse duration in terms of the accelerating gradient. The case of a gas-filled waveguide ICA is analyzed in Sec. VI. The maximum accelerated electron energy imposed by group velocity slippage, i.e., pulse lethargy and ionization, is obtained in Sec. VII. Section VIII presents numerical results for the pulse duration and accelerating gradient, limited by ionization and pulse lethargy, for a 10 μm, 1 mm, and 1 cm wavelength driver in the two ICA configurations. The summary and discussion is given in Sec. IX.

II. FIELDS AND DISPERSION RELATION FOR INVERSE CHERENKOV ACCELERATOR WITH DIELECTRIC LINER

A. Axially symmetric transverse-magnetic mode

The dispersion characteristics of a dielectrically lined waveguide are analyzed in this section. A dielectrically lined waveguide can support an axially symmetric transverse-magnetic mode. The cross-sectional view of the dielectrically lined waveguide is shown in Fig. 1, where the inner surface of the dielectric is at $r = a$ and the conducting outer surface is at $r = b$. The particular TM mode under consideration consists of radial and axial electric fields as well as an azimuthal magnetic field. The field components within the central vacuum region ($0 < r < a$) are

$$E_r = E_0 [J_1(k_\perp r)/J_1(k_\perp a)] f(z,t) + \text{c.c.,} \qquad (1a)$$

$$E_z = i(k_\perp/k) E_0 [J_0(k_\perp r)/J_1(k_\perp a)] f(z,t) + \text{c.c.,} \quad (1b)$$

$$B_\theta = (\omega/ck) E_0 [J_1(k_\perp r)/J_1(k_\perp a)] f(z,t) + \text{c.c.,} \quad (1c)$$

and within the outer dielectric region ($a \leq r \leq b$),

$$E_r = [A J_1(\alpha r) + B Y_1(\alpha r)] f(z,t) + \text{c.c.,} \qquad (2a)$$

$$E_z = i(\alpha/k) [A J_0(\alpha r) + B Y_0(\alpha r)] f(z,t) + \text{c.c.,} \quad (2b)$$

$$B_\theta = \varepsilon(\omega/ck) [A J_1(\alpha r) + B Y_1(\alpha r)] f(z,t) + \text{c.c.,} \quad (2c)$$

where ω is the frequency, k is the axial wave number, $f(z,t) = \frac{1}{2} \exp[i(kz - \omega t)]$, $k_\perp = (\omega^2/c^2 - k^2)^{1/2}$ is the trans-
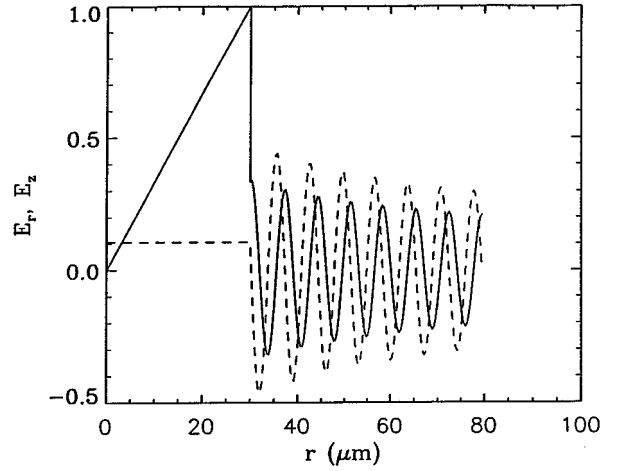

FIG. 2. Axial and radial components of the electric field for a dielectrically lined waveguide supporting an axially symmetric TM mode with phase velocity equal to c. The solid (dotted) curve denotes the radial (axial) component of the electric field normalized to the peak radial field at $r = a$. The parameters are $\lambda = 10$ μm, $a = 30$ μm, $b - a = 50$ μm, and $\varepsilon = 3$.

verse wave number within the inner region, $\alpha = (\varepsilon \omega^2/c^2 - k^2)^{1/2}$ is the transverse wave number within the outer region, ε is the dielectric constant, E_0, A, B are the constant amplitudes, $J_n(x)$ and $Y_n(x)$ are the ordinary Bessel functions of order n and c.c. denotes the complex conjugate. The accelerating axial electric field given by Eq. (1b) is peaked along the z axis.

For application to electron acceleration we will consider the regime where the phase velocity is near c, i.e., $v_{\text{ph}} \equiv \omega/k \cong c$. For phase velocities equal to c, i.e., $k_\perp = 0$, the axial electric field is independent of radial position and given by

$$E_z = i \frac{\lambda}{\pi a} E_0 f(z,t) + \text{c.c.,} \qquad (3)$$

where $\lambda = 2\pi c/\omega$ is the wavelength. The axial and radial components of the electric field for phase velocity equal to c are shown in Fig. 2.

B. Dispersion relation

Applying the appropriate boundary conditions at $r = a$ and b we obtain the following dispersion relation for the TM mode:

$$k_\perp \frac{J_0(k_\perp a)}{J_1(k_\perp a)} = \frac{a}{4} F(\alpha), \qquad (4)$$

where $\alpha^2 = \varepsilon \omega^2/c^2 - k^2 = k_\perp^2 + (\varepsilon - 1)\omega^2/c^2$ and

$$F(\alpha) = \left(\frac{4\alpha}{\varepsilon a}\right) \left(\frac{J_0(\alpha b) Y_0(\alpha a) - J_0(\alpha a) Y_0(\alpha b)}{J_0(\alpha b) Y_1(\alpha a) - J_1(\alpha a) Y_0(\alpha b)}\right).$$

In addition, the amplitudes A and B in terms of E_0 are

$$A = -\frac{E_0}{\varepsilon} \frac{Y_0(\alpha b)}{J_0(\alpha b) Y_1(\alpha a) - J_1(\alpha a) Y_0(\alpha b)}, \qquad (5a)$$

$$B = -AJ_0(\alpha b)/Y_0(\alpha b). \tag{5b}$$

For phase velocities close to c, the dispersion relation can be simplified by taking $k_\perp a$ to be small on the left-hand side of Eq. (4), giving

$$\omega^2/c^2 - k^2 = 8/a^2 - F(\alpha_0), \tag{6}$$

where $\alpha_0 = (\varepsilon - 1)^{1/2}\omega/c$. In obtaining Eq. (6) the small argument forms $J_0(x) \cong 1 - x^2/4$ and $J_1(x) \cong x/2 - x^3/16$ were used.

The dispersion relation in Eq. (6), which is valid for phase velocities near c, can be further simplified by considering several limiting regimes. A relevant regime corresponds to the limit where the waveguide is large and/or the dielectric constant is far from unity, corresponding to the inequality $\alpha_0 a \gg 1$, i.e.,

$$\lambda/a \ll 2\pi(\varepsilon - 1)^{1/2}. \tag{7}$$

The dispersion relation in this regime is given by

$$\omega^2/c^2 - k^2 = 8/a^2 - \frac{4\alpha_0}{\varepsilon a}\tan[\alpha_0(b - a)]. \tag{8}$$

In obtaining Eq. (8) the asymptotic form $F(\alpha_0) = (4\alpha_0/\varepsilon a)\tan[\alpha_0(b-a)]$ has been used. The components of the electric field within the dielectric are

$$\begin{pmatrix} E_r \\ E_z \end{pmatrix} \approx E_0\left(\frac{a}{r}\right)^{1/2}\begin{cases} \varepsilon^{-1}\dfrac{\cos[\alpha_0(b-r)]}{\cos[\alpha_0(b-a)]}f(z,t) + \text{c.c.} & \text{(9a)} \\[4mm] \dfrac{i\lambda}{\pi a}\dfrac{\sin[\alpha_0(b-r)]}{\sin[\alpha_0(b-a)]}f(z,t) + \text{c.c.} & \text{(9b)} \end{cases}$$

The dispersion relation in Eq. (8) can be solved explicitly in three cases. To obtain the frequencies associated with these cases it is convenient to rewrite the dispersion relation in Eq. (8), for phase velocities equal to c, in the form

$$\tan \xi = 2\varepsilon(b-a)/(a\xi), \tag{10}$$

where $\xi = \alpha_0(b-a)$. In case 1 the right-hand side of Eq. (10) is much greater than unity, i.e., $\lambda/a \gg \pi(\varepsilon-1)^{1/2}/\varepsilon$, and $\xi \approx (l+1/2)\pi$, where $l = 0,1,2,\ldots$. This case is compatible with the inequality in Eq. (7) provided ε is sufficiently large compared to unity. In case 2 the right-hand side is small compared to unity, i.e., $\lambda/a \ll \pi(\varepsilon-1)^{1/2}/\varepsilon$, and $\xi \approx l\pi$, where l is a large integer. Note that the inequality defining this case is more restrictive than that in Eq. (7). Finally, case 3 corresponds to $\xi \ll 1$, i.e., when the liner is very thin, $(b-a)/\lambda \ll (\varepsilon-1)^{-1/2}/(2\pi)$. We emphasize that the inequality in Eq. (7) applies to all three cases. The wavelengths associated with these cases are obtained from Eq. (10),

$$\frac{\lambda}{a} \approx 2\frac{b-a}{a}(\varepsilon-1)^{1/2}\begin{cases} (l+1/2)^{-1} & \text{(11a)} \\[3mm] l^{-1} & \text{(11b)} \\[3mm] \dfrac{\pi}{(2\varepsilon)^{1/2}}\left(\dfrac{a}{b-a}\right)^{1/2}, & \text{(11c)} \end{cases}$$

where Eq. (11a) corresponds to case 1 with l nodes in the liner, Eq. (11b) corresponds to case 2 with l nodes in the liner, and Eq. (11c) corresponds to case 3 with no nodes in the liner. The radial component of the electric field inside the dielectric material is given by

$$E_r \approx \frac{E_0}{\varepsilon}\left(\frac{a}{r}\right)^{1/2}\begin{cases} (-1)^l(\lambda/\pi a)[\varepsilon/(\varepsilon-1)^{1/2}]\cos\left(\xi\dfrac{b-r}{b-a}\right)f(z,t) + \text{c.c.} & \text{(12a)} \\[4mm] (-1)^l\cos\left(\xi\dfrac{b-r}{b-a}\right)f(z,t) + \text{c.c.} & \text{(12b)} \\[4mm] f(z,t) + \text{c.c.}, & \text{(12c)} \end{cases}$$

where ξ in Eqs. (12a) and (12b) is given by Eq. (10) in the appropriate limit. Similarly, the axial components of the electric field inside the dielectric liner are given by

$$E_z \approx E_0\left(\frac{a}{r}\right)^{1/2}\frac{i\lambda}{\pi a}\begin{cases} (-1)^l\sin\left(\xi\dfrac{b-r}{b-a}\right)f(z,t) + \text{c.c.} & \text{(13a)} \\[4mm] (-1)^l(\pi a/\lambda)[(\varepsilon-1)^{1/2}/\varepsilon]\sin\left(\xi\dfrac{b-r}{b-a}\right)f(z,t) + \text{c.c.} & \text{(13b)} \\[4mm] \dfrac{b-r}{b-a}f(z,t) + \text{c.c.} & \text{(13c)} \end{cases}$$

Using these expressions one can readily verify that the field components satisfy the appropriate continuity and boundary conditions at the surface of the liner ($r = a$) and at the conducting wall ($r = b$).

Other regimes of the dispersion relation in Eq. (6) can be evaluated but do not lead to phase velocities equal to c. Simplification of the dispersion relation in Eq. (6) in the regime of long wavelengths may be made by taking $\alpha_0 b \ll 1$, i.e., $\lambda/b \gg 2\pi(\varepsilon-1)^{1/2}$. This regime is incompatible with phase velocities equal to c, as is shown below. The dispersion relation, in this regime, takes the form

$$\omega^2/c^2 - k^2 = 8/a^2 - \varepsilon^{-1}(2\alpha_0)^2 \log_e(b/a).$$

The solution of this dispersion relation when the phase velocity is equal to c can be written in the form

$$\frac{\lambda}{b} = 2\pi(\varepsilon-1)^{1/2}\left(\frac{a/b}{2\varepsilon}\right)^{1/2}\left[\frac{\log_e(b/a)}{b/a}\right]^{1/2}.$$

To be consistent with the inequality defining this regime we require $\lambda/[2\pi b(\varepsilon-1)^{1/2}] \gg 1$, which is impossible since $b > a$ and $\varepsilon > 1$. Hence there is no solution to the dispersion relation as λ becomes large compared to the dimensions of the outer conductor. The final regime that we identify explicitly corresponds to $\alpha_0 a \ll 1$ and $\alpha_0 b \gg 1$. Again this regime is incompatible with phase velocities equal to c since the dispersion relation reduces to $2\varepsilon = -(\alpha_0 a)^2 \log_e(\alpha_0 a)$. In the limit $\alpha_0 \to 0$, the right-hand side vanishes and hence no solution to the dispersion relation exists.

III. CRITICAL AVERAGE PLASMA DENSITY

The large fields needed for acceleration can ionize the dielectric material and change the dispersive properties of the waveguide. If the dispersive properties change sufficiently phase velocity slippage will occur and the acceleration will cease. As ionization takes place the dielectric constant from ε to $\varepsilon + \delta\varepsilon$, where $\delta\varepsilon = -\omega_p^2/\omega^2$ is the contribution to the dielectric constant due to ionization, $\omega_p = (4\pi q^2 \langle n_p\rangle/m)^{1/2}$ is the average plasma frequency, q is the charge and m is the mass of an electron, and $\langle n_p\rangle$ is the average plasma density within the waveguide, i.e., $\langle n_p\rangle$ is the peak plasma density times the ratio of the cross-sectional area of the plasma to the cross-sectional area of the waveguide. When the change in $F(\alpha_0)$ in Eq. (6) due to ionization equals $\sim 8/a^2$, the optical properties of the guide change significantly and phase velocity slippage disrupts the acceleration. Ionization in the dielectric material will not disrupt the acceleration provided

$$|\delta\varepsilon| = \omega_p^2/\omega^2 \ll (8/a^2)|\partial F/\partial\varepsilon|^{-1}. \tag{14}$$

This inequality defines a critical average plasma density within the dielectric, $n_{\rm crit}$, given by

$$n_{\rm crit} = \frac{2}{\pi r_e}\left(\frac{\omega/c}{a}\right)^2 |\partial F/\partial\varepsilon|^{-1}, \tag{15}$$

where $r_e = q^2/mc^2 = 2.8 \times 10^{-13}$ cm is the classical electron radius. If the average plasma density $\langle n_p\rangle$ generated within the dielectric exceeds $n_{\rm crit}$ the acceleration is disrupted because of phase velocity slippage.

The critical average plasma density can be evaluated in the limiting cases discussed in connection with the dispersion relation in Sec. II. The critical average plasma density in the three cases is

$$n_{\rm crit} = \frac{\varepsilon^2}{2\pi}\frac{1}{a^2 r_e}\frac{a}{b-a}\begin{cases}\left(\dfrac{\pi^2}{2\varepsilon^3}\right)\left(\dfrac{a}{b-a}\right)^2(l+\tfrac{1}{2})^2 & \text{(16a)}\\[2mm] 2\varepsilon^{-1} & \text{(16b)}\\[2mm] 1, & \text{(16c)}\end{cases}$$

where Eqs. (16a)–(16c) refer to cases 1–3, respectively. As an illustration we take $\varepsilon = 2$, $a = 100$ μm, $a/(b-a) = 2$ and find that the critical density for phase slippage in case 2 is $n_{\rm crit} \cong 5 \times 10^{16}$ cm^{-3}, and is independent of the wavelength. For a 10 μm wavelength, this value is more than two orders of magnitude smaller than the plasma density for complete reflection ($\sim 10^{19}$ cm^{-3}).

IV. IONIZATION IN SOLIDS

The rate of change of plasma density (density of free electrons) is given by

$$\frac{\partial n_p}{\partial t} = S + W n_p - \nu_r n_p, \tag{17}$$

where S is the photoionization source due to electron tunneling, W is the collisional ionization rate, and ν_r is the recombination rate. The photoionization source acts as an initial source of free electrons which are further increased in number by collisional processes, i.e., by electron avalanche. Typically, for parameters of interest here, the recombination rate is small compared to the collisional ionization rate, i.e., $\nu_r < W$, and will be neglected. Note that S and W have units of sec^{-1} cm^{-3} and sec^{-1}, respectively, and will be specified later. The solution of Eq. (17) is

$$n_p = (S/W)[\exp(Wt) - 1] + n_{p0}\exp(Wt), \tag{18}$$

where n_{p0} is the seed electron density and it is assumed that the plasma density remains small compared to the neutral density.

A. Collisional ionization

The collisional ionization rate can be estimated by using a classical free electron model for the electron energy gain. The rate of change of energy of an electron undergoing collisions in the presence of a temporally periodic electric field is given by [21,22]

$$\frac{dU}{dt} = \frac{q^2 E^2 \nu_m}{2m(\omega^2 + \nu_m^2)} - \frac{2m}{M}\nu_m U, \tag{19}$$

where U is the electron energy, E is the peak electric field amplitude, ν_m is the momentum transfer frequency, and M is the mass of the neutral atoms. The first term on the right-hand side of Eq. (19) represents the rate of energy increase of an electron undergoing collisions while being accelerated in the alternating field. The second term represents the energy damping due to inelastic collisions between electrons and neutral atoms. Note that E in Eq. (19) refers to the peak

electric field in the dielectric. Equation (19) indicates that the electron energy increases monotonically and saturates because of inelastic electron collisions with neutral atoms. Solving Eq. (19), we obtain

$$U(t) = U_{\text{sat}}[1 - \exp(-\nu_0 t)], \tag{20}$$

where $U_{\text{sat}} = (\nu_m/\nu_0)(1 + \nu_m^2/\omega^2)^{-1} U_{0s}$ is the saturation (maximum) electron energy, $U_{0s} = m v_{0s}^2/2$ is the electron oscillation energy, $v_{0s} = qE/m\omega$ is the oscillation velocity, and $\nu_0 = 2m\nu_m/M$ is the energy damping frequency. Typically, in solids $\nu_m \sim 10^{15}$ sec^{-1} [23] and $\nu_0 \sim 10^{11}$ sec^{-1}. When the electron energy reaches the ionization energy U_I, the electron collisionally ionizes the atom. The time for this to occur is the ionization time W^{-1}. Setting $U = U_I$ and $t = W^{-1}$ in Eq. (20) determines W,

$$W = -\nu_0/\log_e(1 - U_I/U_{\text{sat}}), \tag{21}$$

for $U_I/U_{\text{sat}} < 1$ and $W = 0$ for $U_I/U_{\text{sat}} > 1$. For $U_I/U_{\text{sat}} \ll 1$, Eq. (21) becomes $W \cong (U_{0s}/U_I)\nu_m/(\nu_m^2/\omega^2 + 1)$. Note that $(U_I/U_{0s})^{1/2} = \gamma_k$ is the Keldysh parameter [24] and $\gamma_k < 1$ corresponds to the tunneling ionization regime. As noted earlier, we assume that the ionization takes place within the dielectric material. The minimum electric field for ionization, associated with long pulses, can be estimated from Eq. (20) by taking $U(t \to \infty) = U_I$:

$$\widetilde{E} = (2m/M)^{1/2}[(\omega^2 + \nu_m^2)^{1/2}/\Omega_0]\widetilde{U}_I^{1/2}, \tag{22}$$

where $\widetilde{U}_I = U_I/U_{\text{H}}$ is the atomic ionization energy U_I normalized to that of hydrogen, $U_{\text{H}} = q^2/(2a_0) = 13.6$ eV, $\widetilde{E} = E/E_{\text{H}}$ is the peak electric field normalized to the hydrogenic electric field $E_{\text{H}} = |q|/a_0^2 = 5.2$ GV/cm, $\Omega_0 = 4\pi U_{\text{H}}/h = 4.1 \times 10^{16}$ sec^{-1} is the atomic frequency, $a_0 = (h/2\pi q)^2/m = 5.3 \times 10^{-9}$ cm is the Bohr radius, and h is Planck's constant. Irregularities on the surface of the dielectric liner may permit surface plasma formation at electric field amplitudes substantially smaller than that implied by Eq. (22). The results, in this paper, for maximum accelerating fields are therefore expected to be upper bound estimates. The rough estimate for the collisional ionization rate in Eq. (21) is used, together with the tunneling source term S, to obtain the plasma density in Eq. (18).

B. Tunneling ionization source

The ionization source in solids, averaged over times much longer than the field period $2\pi/\omega$, in the tunneling regime $\gamma_k = (U_I/U_{0s})^{1/2} < 1$, is given by [25]

$$S = A_s \widetilde{E}^{5/2} \exp[-\beta_s/\widetilde{E}], \tag{23}$$

where

$$A_s = 1.5 \times 10^{40}/\widetilde{U}_I^{5/4}, \tag{24a}$$

$$\beta_s = 0.56\widetilde{U}_I^{3/2}. \tag{24b}$$

In Eqs. (23) and (24), A_s has units of sec^{-1} cm^{-3}.

Figure 3 shows the tunneling ionization source term and the collisional ionization rate as functions of the normalized
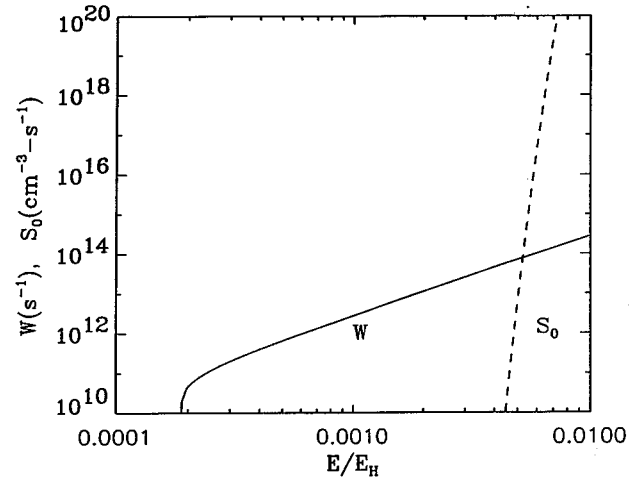

FIG. 3. Plot of tunneling ionization source function S and collisional ionization rate W as a function of normalized electric field $\widetilde{E} = E/E_{\text{H}}$. In this plot $U_I = 8$ eV, $\lambda = 10$ μm, $\nu_m = 10^{15}$ sec^{-1}, and $\nu_0 = 10^{11}$ sec^{-1}.

electric field. For pulses that are shorter than a few picoseconds, collisional ionization is negligible for $W < 10^{10}$ sec^{-1}. The precipitous drop in W below $\widetilde{E} = 2 \times 10^{-4}$ occurs as U_{max} approaches U_1 in Eq. (21). The tunneling term S does not lead to significant ionization for $\widetilde{E} < 5 \times 10^{-3}$, but ionization increases rapidly for higher fields.

V. LIMITATION ON LASER PULSE DURATION AND ACCELERATING GRADIENT

To avoid modifying the dispersive properties of the waveguide the average induced plasma density must be less than the critical average density n_{crit}, i.e., $\langle n_p \rangle \ll n_{\text{crit}}$. Using Eq. (18) for n_p we find that

$$\langle n_p \rangle = \langle (S/W)[\exp(W\tau_L) - 1] \rangle + n_{p0}\langle \exp(W\tau_L) \rangle \ll n_{\text{crit}}, \tag{25}$$

where $\langle \rangle$ denotes the average over the cross-sectional area of the waveguide and τ_L is the laser pulse duration. The average plasma density in Eq. (25) consists of a tunneling and collisional ionization term and a contribution from the seed electron density. To perform the cross-sectional average we note that in the ionization part, the source function S is a highly sensitive function of the field amplitude through the exponential dependence on the field [see Eq. (23)]. Because of this sensitivity, the spatial average of the ionization term in Eq. (25) is applied only to the function S while the collisional ionization rate W is evaluated at the peak field amplitude. The cross-sectional average of the contribution from the initial plasma electron density can be written as $\langle \exp(W\tau_L) \rangle \cong f \exp(W_m\tau_L)$ where f is a filling factor due to the spatial variation of the field within the dielectric. Employing these approximations, Eq. (25) becomes

$$W_m^{-1}[\exp(W_m\tau_L) - 1]\langle S \rangle + f n_{p0}\exp(W_m\tau_L) \ll n_{\text{crit}}, \tag{26}$$

where W_m is the maximum value of W, i.e., W evaluated at the peak electric field E_m inside the dielectric. The filling factor f is found to be given by

$$f \cong \begin{cases} \frac{1}{2} & (27a) \\ (\pi/8)^{1/2}(W_m\tau_L)^{-1/2} & (27b) \\ 2(b-a)/b, & (27c) \end{cases}$$

where Eq. (27a) refers to either case 1 or case 2 when $W_m\tau_L \ll 1$, Eq. (27b) refers to either case 1 or case 2 when $W_m\tau_L \gg 1$, and Eq. (27c) refers to only case 3.

The pulse duration of the driver in the ICA must not exceed a critical pulse duration τ_{crit}. Substituting Eq. (16) into Eq. (26) we obtain the following inequality on the pulse duration;

$$\tau_L \ll \tau_{\text{crit}} = W_m^{-1}\log_e[(\tau_0 W_m + 1)/(1 + fn_{p0}W_m/\langle S\rangle)], \quad (28)$$

where $\tau_0 = n_{\text{crit}}/\langle S\rangle$. If the laser pulse duration is small compared to the collisional ionization time, i.e., $\tau_L \ll W_m^{-1}$, and the initial plasma density is zero, $n_{p0}=0$, the inequality in Eq. (28) becomes $\tau_L \ll \tau_0 = n_{\text{crit}}/\langle S\rangle$. The inequality in Eq. (28) places a limit on the pulse duration, which is a function of the accelerating gradient, $E_z = (\lambda/a\pi)E_0$. If the pulse duration exceeds the value given by Eq. (28), sufficient ionization will take place to modify the dispersive properties of the waveguide, causing phase velocity slippage to terminate the acceleration.

The critical time τ_{crit} in Eq. (28) must be determined explicitly for the three cases. The average ionization source term is

$$\langle S\rangle \cong 2\pi \int_a^b Sr\, dr/(\pi b^2), \quad (29)$$

where the radial variation in S arises from that of the electric field. Since the ionization source term S is a highly sensitive function of the electric field due to the exponential factor in Eq. (23), the integral in Eq. (29) can be approximately evaluated. In the limit defined by the inequality in Eq. (7) the electric field is given by Eqs. (12) and (13). Making use of these expressions in Eq. (29) and expanding about each of the l peaks for case 1 or 2, and about the peak at $r=a$ for case 3, we obtain

$$\langle S\rangle \cong \frac{a^2}{2b^2}S_m \begin{cases} \pi^{1/2}\dfrac{(b-a)}{a}(\widetilde{E}_m/\beta_s)^{1/2}, & (30a) \\ 8\widetilde{E}_m/\beta_s, & (30b) \end{cases}$$

where Eq. (30a) refers to either case 1 or case 2 and Eq. (30b) refers to only case 3 and S_m is S evaluated at $\widetilde{E}_m = E_m/E_H$, i.e.,

$$S_m = A_s\widetilde{E}_m^{5/2}\exp[-\beta_s/\widetilde{E}_m]. \quad (31)$$

Using Eq. (30) for $\langle S\rangle$ and Eq. (18) for n_{crit}, we obtain

$$\tau_0 = n_{\text{crit}}/\langle S\rangle = \frac{\varepsilon^2}{8\pi}\frac{1}{a^2 r_e}\frac{a}{b-a}\frac{b^2}{a^2 S_m}$$

$$\times \begin{cases} \left(\dfrac{a/\varepsilon}{b-a}\right)^3(2l+1)^2(\pi^3\beta_s/\widetilde{E}_m)^{1/2} & (32a) \\ \dfrac{16}{\pi^{1/2}\varepsilon}\dfrac{a}{b-a}(\beta_s/\widetilde{E}_m)^{1/2} & (32b) \\ \beta_s/\widetilde{E}_m, & (32c) \end{cases}$$

where Eq. (32a) refers to case 1, Eq. (32b) refers to case 2, and Eq. (32c) refers to case 3. From Eq. (28), values of τ_0 for the various cases can be used to determine the limits on the pulse duration and the accelerating gradient.

VI. GAS-FILLED INVERSE CHERENKOV ACCELERATOR

Another configuration for the inverse Cherenkov accelerator consists of a waveguide that is filled with a neutral gas. The presence of the neutral gas modifies the electromagnetic properties of the waveguide, making the phase velocity of the accelerating electric field equal to the speed of light. For sufficiently low gas densities, the collisional scattering of the accelerated electrons can be neglected [26].

In this section we consider the limitations on electromagnetic pulse duration and accelerating gradient of an ICA consisting of a gas-filled cylindrical waveguide of radius a. For the TM mode the fields are given by Eq. (1), with $k_\perp = (\varepsilon\omega^2/c^2 - k^2)^{1/2}$, where $\varepsilon \gtrsim 1$ is the dielectric constant of the gas. The dispersion relation for the TM mode is given by $k_\perp a = p_{0n}$, or

$$\varepsilon\omega^2/c^2 - k^2 = (p_{0n}/a)^2, \quad (33)$$

where p_{0n} is the nth zero of J_0. Writing $\varepsilon = 1 + \Delta\varepsilon$, where $\Delta\varepsilon > 0$ is the contribution of the neutral gas to the dielectric constant, from Eq. (33) we find that, for the phase velocity to equal c, the wavelength is given by

$$\lambda/a = (2\pi/p_{0n})\Delta\varepsilon^{1/2}. \quad (34)$$

Since $\Delta\varepsilon \ll 1$ for gases at moderate pressures, i.e., a few atmospheres, the expression in Eq. (34) implies that $\lambda/a \ll 1$. Noting that $E_z = (\lambda/\pi a)E_0$ on axis, the accelerating field is necessarily small compared to the field amplitude E_0.

To determine the critical average plasma density n_{crit} in the gas-filled ICA, we proceed as in Sec. III. Accounting for the ionization of the ambient gas, we write $\varepsilon = 1 + \Delta\varepsilon - \omega_p^2/\omega^2$ and obtain the critical plasma density

$$n_{\text{crit}} = \pi\Delta\varepsilon/(r_e\lambda^2) = p_{0n}^2/4\pi a^2 r_e. \quad (35)$$

Typically $\Delta\varepsilon \sim 10^{-4}$ for a gas at atmospheric pressure, and for a $\lambda = 10$ μm laser-driven gas-filled ICA, the critical density is found to be $n_{\text{crit}} \cong 10^{15}$ cm^3.

The development of plasma in the gas, undergoing ionization due to tunneling and collisional processes, is given by Eq. (17). The ionization source term in Eq. (17) for a gas is given by [24]

$$S = A_g\widetilde{E}^{-1/2}\exp(-\beta_g/\widetilde{E}), \quad (36)$$

where

$$A_g = 1.6 \times 10^{17} \widetilde{U}_I^{7/4} n_{n0}, \qquad (37a)$$

$$\beta_g = 0.67 \widetilde{U}_I^{3/2}, \qquad (37b)$$

n_{n0} is the neutral gas density in units of cm^{-3}, and A_g in Eq. (37a) is in units of $sec^{-1}\, cm^{-3}$. The collisional ionization rate W is given by Eq. (21). Similarly, the rate of change of electron energy is given by Eq. (19), where, the momentum transfer frequency ν_m in a gas is proportional to the pressure and is on the order of $10^{12}\ sec^{-1}$ at atmospheric pressure [21,22]. The limitation of the pulse duration and accelerating gradient in the gas-filled ICA is given by Eq. (28). For a gas-filled ICA, $\tau_0 = n_{crit}/\langle S \rangle$, where n_{crit} is given by Eq. (35), $\langle S \rangle$ is

$$\langle S \rangle \cong S_m (2\pi \widetilde{E}_m / \beta_g)^{1/2}, \qquad (38)$$

and S_m is the value of S evaluated at peak electric field E_0, i.e., $\widetilde{E}_0 = E_m / E_H$. The filling factor f in Eq. (28) for the gas-filled waveguide ICA is

$$f \cong \begin{cases} \frac{1}{2} \\ (\pi/2)^{1/2} (W_m \tau_L)^{-1/2}, \end{cases} \qquad (39)$$

where the upper (lower) value is for $W_m \tau_L \ll 1$ $(\gg 1)$.

VII. GROUP VELOCITY SLIPPAGE (PULSE LETHARGY)

Ionization effects place an upper limit on the pulse duration of the electromagnetic driver, see Eq. (28). Group velocity slippage or pulse lethargy, on the other hand, places a lower limit on the pulse duration of the driver. That is, the distance the pulse slips behind the accelerated electrons must be less than the pulse length,

$$(v_g^{-1} - c^{-1})L < \tau_L, \qquad (40)$$

where v_g is the group velocity and L is the propagation distance. Using Eq. (8) the group velocity $v_g \equiv \partial \omega / \partial k$ is given by

$$v_g = c\, \frac{1 + (\lambda/4\pi)(\varepsilon-1)^{-1/2} \partial F/\partial \alpha_0}{1 + (\lambda/4\pi)\varepsilon(\varepsilon-1)^{-1/2} \partial F/\partial \alpha_0}, \qquad (41)$$

where $F = (4\alpha_0 / \varepsilon a)\tan[\alpha_0(b-a)]$. Making use of Eq. (41), the group velocity in the three cases is given by

$$v_g/c \approx \begin{cases} 1/\varepsilon & (42a) \\ \dfrac{1 + 2(b-a)/(\varepsilon a)}{1 + 2(b-a)/a} & (42b) \\ \dfrac{1 + 4(b-a)/(\varepsilon a)}{1 + 4(b-a)/a}. & (42c) \end{cases}$$

Note that Eq. (42a), which corresponds to case 1, indicates that the group velocity $\approx c/\varepsilon$. This is consistent with the relationship $v_{ph} v_g = c^2/\varepsilon$ for a completely filled waveguide. Substituting Eq. (42) into Eq. (40) yields the limit on the interaction length due to pulse lethargy,

$$L < G(\varepsilon, a, b) c \tau_L, \qquad (43)$$

where

$$G = (\varepsilon - 1)^{-1} \begin{cases} 1 & (44a) \\ 1 + \varepsilon a/2(b-a) & (44b) \\ 1 + \varepsilon a/4(b-a). & (44c) \end{cases}$$

In obtaining Eq. (41) we have neglected the effects of the induced plasma, i.e., $\omega_p = 0$. For a gas-filled ICA, discussed in Sec. VI, the group velocity, neglecting transverse effects, is given by $v_g/c \approx \varepsilon^{-1}$, which, upon substitution into Eq. (40) yields the limit on the interaction length,

$$L < (\varepsilon - 1)^{-1} c \tau_L, \qquad (45)$$

which is identical in form to case 1, Eq. (44a), of the dielectrically lined configuration.

The limitation on the pulse length due to ionization, Eq. (28), together with the limitations imposed by pulse lethargy, Eqs. (43), present a severe constraint on the interaction length, and therefore the maximum energy gain, in the ICA. The limitation on the interaction length L can be stated in terms of the maximum electron energy U_{max} and the acceleration gradient E_z. In practical units the maximum electron energy gain in the ICA in terms of the acceleration gradient and pulse duration is

$$U_{max}[MeV] < 3 \times 10^8 G(\varepsilon, a, b) E_z[MV/m]\, \tau_L[sec], \qquad (46)$$

where the values of E_z and τ_L are obtained from Eq. (28). Using Eq. (28) the pulse duration in Eq. (46) can be written in terms of the accelerating gradient. Hence the maximum electron energy, given by Eq. (46), can be expressed in terms of only the accelerating gradient.

VIII. RESULTS

We first describe the results for the ICA configuration with a dielectric liner for three wavelength drivers, $\lambda = 10\ \mu m$, 1 mm, and 1 cm. The plots principally show the scaling of the critical time with the accelerating gradient as the parameters are varied. The minimum value of τ_{crit} shown in all the figures corresponds to a pulse duration of 30 wave periods. Technological issues as well as longitudinal dispersion limit the pulse duration to several tens of wave periods. For a $\lambda = 10\ \mu m$, 1 mm, and 1 cm wavelength driver, the minimum value of τ_{crit} used in the figures is 1 psec, 0.1 nsec, and 1 nsec, respectively.

Figure 4 is a plot of the critical time as a function of the accelerating gradient, for $\lambda = 10\ \mu m$, as the inner radius of the waveguide is varied. The dielectric layer thickness $b - a = 50\ \mu m$ in all three cases, with $a = 30$, 50, and 100 μm for the three curves. Figure 5 shows the variation of τ_{crit} as a function of E_z, for $\lambda = 10\ \mu m$, for various values of initial electron density in the dielectric liner. The addition of a small number of electrons to seed the collisional ionization process reduces the allowable accelerating gradient E_z for a given value of τ_{crit}. Figure 6 shows the variation of τ_{crit} versus the accelerating gradient, for $\lambda = 10\ \mu m$, for several values of ionization energy associated with the dielectric liner material. For a given critical pulse time τ_{crit}, higher ionization potentials permit higher accelerating gradients.
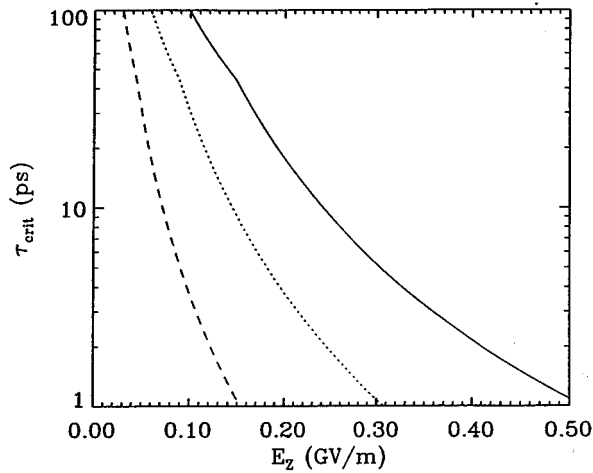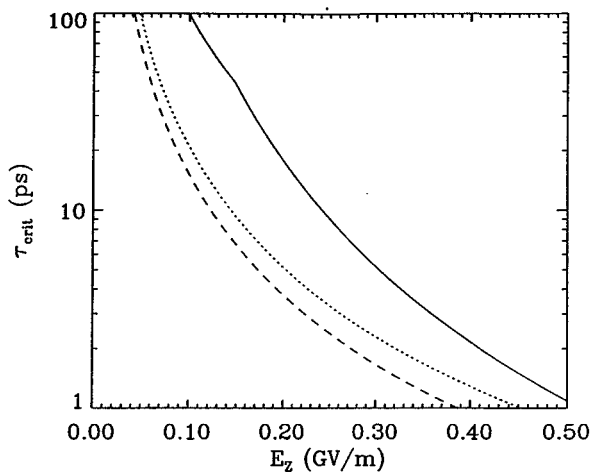
FIG. 4. Plot of critical pulse time τ_{crit} versus the accelerating gradient E_z for a laser of wavelength $\lambda = 10$ μm, inner radius $a = 30$ μm (solid curve), 50 μm (dotted curve), and 100 μm (dashed curve), $b - a = 50$ μm. In addition, $\varepsilon = 3$, $U_I = 8$ eV, $n_{p0} = 0$, $\nu_m = 10^{15}$ sec^{-1}, and $\nu_0 = 10^{11}$ sec^{-1}.

Figure 7 plots the critical time as a function of the accelerating gradient, for $\lambda = 10$ μm, as the dielectric constant ε is varied. As the dielectric constant is increased, the electric field in the dielectric decreases (to maintain continuity of the displacement field εE_r across the vacuum-dielectric boundary), and thus the ionization level is reduced. It should be noted, however, that for high values of ε, ionization is likely to occur at the surface rather than in the bulk of the dielectric layer, and thus the high gradients predicted for large values of ε result in surface breakdown.

Figure 8 is a plot of the maximum electron energy U_{max} as a function of the accelerating gradient E_z from Eq. (46). In obtaining this plot the driver pulse duration τ_L is set equal to τ_{crit} given by Fig. 4. For energy gains above U_{max} ~ 10 MeV, Fig. 8 indicates that the accelerating gradient is

limited to $E_z \sim 20$ MV/m. This rather low value of accelerating gradient corresponds to the onset of collisional ionization (see Fig. 3) for these parameters.

We now consider the example of a millimeter wave driver. Figure 9 shows the variation of τ_{crit} with E_z, for $\lambda = 1$ mm, as the radius of the inner wall radius is varied. The scaling here is similar to the $\lambda = 10$ μm case shown in Fig. 4, but the allowable accelerating gradient is lower. The longer pulse lengths, compared to the 10 μm wavelength example, are the principle reason for the lower accelerating gradients. Recall that the minimum value of τ_{crit}, in all the examples, is taken to be equal to 30 wave periods of the driving field. This is an arbitrary but technologically reasonable lower limit on the pulse duration. Figure 10 is a plot of τ_{crit} versus E_z for $\lambda = 1$ mm, as the seed electron density is varied. This case is similar to the $\lambda = 10$ μm case shown in Fig. 5. The
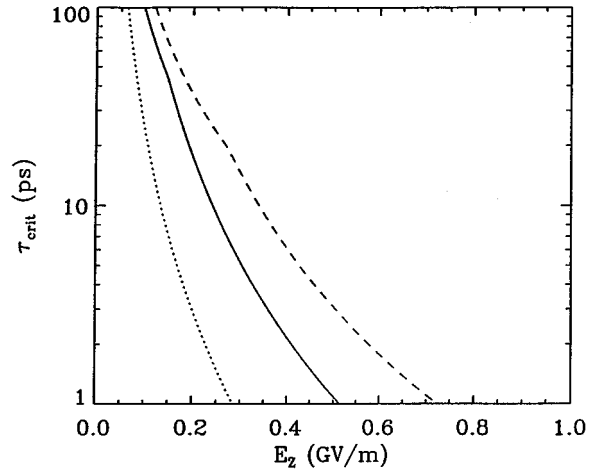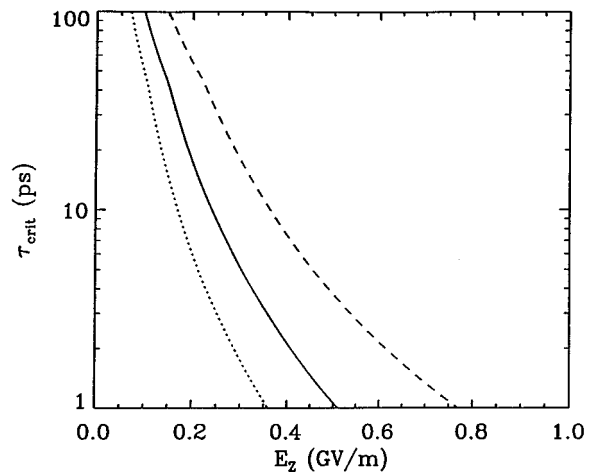

FIG. 6. Plot of critical pulse time τ_{crit} versus the accelerating gradient E_z for a laser of wavelength $\lambda = 10$ μm. The ionization potential $U_1 = 4$ eV (dotted curve), 8 eV (solid curve), 12 eV (dashed curve). The other parameters are the same as in Fig. 5 with $n_{p0} = 0$.

FIG. 5. Plot of critical pulse time τ_{crit} versus the accelerating gradient E_z for a laser of wavelength $\lambda = 10$ μm. The initial electron density n_{p0} is 0 (solid curve), 1 cm^{-3} (dotted curve), and 10^5 cm^{-3} (dashed curve). In addition, $a = 30$ μm, $b = 80$ μm, $\varepsilon = 3$, $U_I = 8$ eV, $\nu_m = 10^{15}$ sec^{-1}, and $\nu_0 = 10^{11}$ sec^{-1}.

FIG. 7. Plot of critical pulse time τ_{crit} versus the accelerating gradient E_z for a laser of wavelength $\lambda = 10$ μm. The dielectric constant $\varepsilon = 1.5$ (dotted curve), 3 (solid curve), 9 (dashed curve). The other parameters are the same as in Fig. 6 with $U_I = 8$ eV.

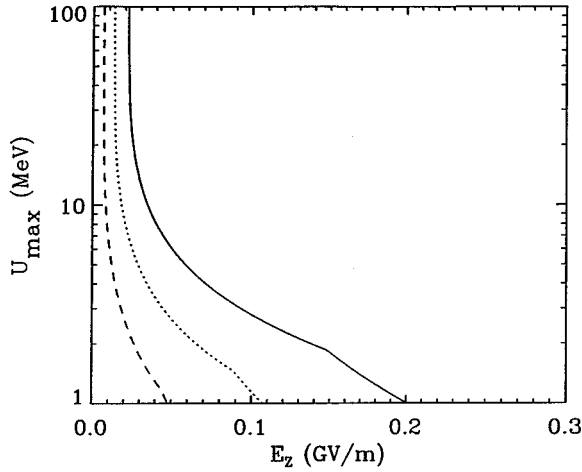FIG. 8. Plot of maximum electron energy versus accelerating gradient for the parameters in Fig. 4 with $a = 30$ μm (solid curve), 50 μm (dotted curve), and 100 μm (dashed curve).

addition of a small amount of seed electrons reduces the accelerating gradient significantly. A case 1 example is shown in the next figure, where the driver wavelength is larger than the inner dielectric radius, $\lambda > a$. Figure 11 shows τ_{crit} versus E_z for $\lambda = 1$ mm and initial (seed) electron density $n_{p0} = 0$ and 1 cm^{-3}. The lower limit on E_z is due to the sudden turn on of collisional ionization rate W as a function of electric field, see Fig. 3. Figure 12 shows the maximum electron energy U_{max} as a function of the accelerating gradient E_z for the millimeter wave example in Fig. 9. Figure 12 indicates that for energy gains in excess of $U_{\mathrm{max}} \sim 20$ MeV the accelerating gradient is less than $E_z \sim 20$ MV/m.

The solid curve in Fig. 13 shows τ_{crit} versus E_z for a driver wavelength of $\lambda = 1$ cm and $a = 0.2$ cm, corresponding to case 1. The dashed curve in Fig. 13 shows the maximum electron energy U_{max} as a function of the accelerating gradient E_z. Figure 13 indicates that for energy gains above
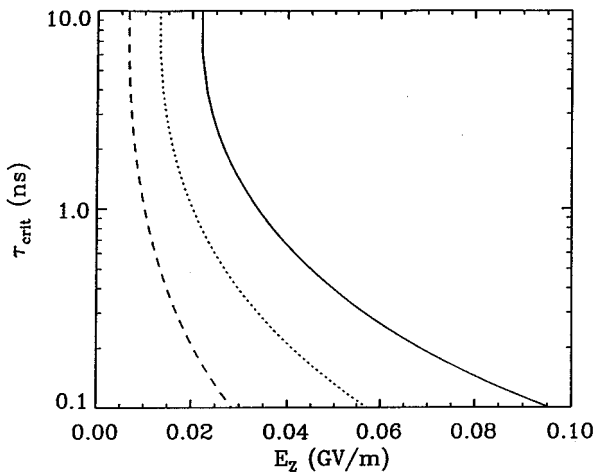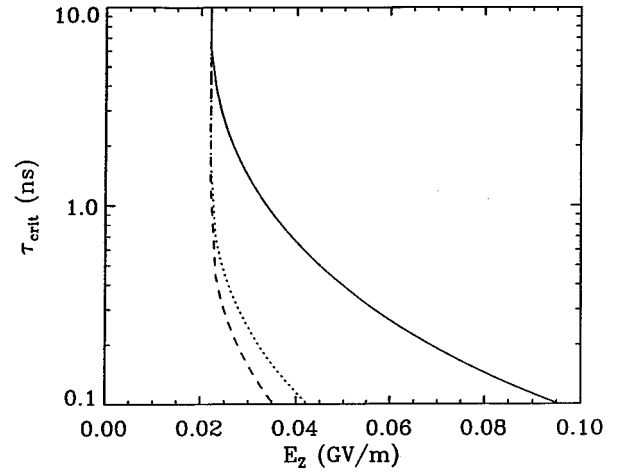

FIG. 10. Plot of critical pulse time τ_{crit} versus the accelerating gradient E_z for a millimeter wave driver, $\lambda = 1$ mm. The initial electron density n_{p0} is 0 (solid curve), 1 cm^{-3}, (dotted curve), and 10^5 cm^{-3} (dashed curve). The parameters are the same as in Fig. 9, with $a = 3$ mm and $b = 8$ mm.

$U_{\mathrm{max}} \sim 10$ MeV the accelerating gradient is less than $E_z \sim 100$ MV/m, due to the onset of collisional ionization.

Figures 14 and 15 show the critical pulse duration τ_{crit} versus the accelerating gradient E_z for a gas-filled ICA. The gas is taken to be helium having an ionization potential of $U_I = 24.6$ eV. The variation of the critical time τ_{crit} with the accelerating gradient E_z, at $\lambda = 10$ μm, is shown for gas pressures P_g of 3, 10, and 30 atm. Since $\varepsilon - 1 = \Delta \varepsilon = 7 \times 10^{-5}$ at 1 atm for helium, the dispersion relation for the lowest order mode, $p_{0n} = 2.4$, gives $a = 265$, 145, and 84 μm, respectively, for the three pressures. This gas-filled case has a lower accelerating gradient than the dielectric liner case shown in Fig. 4, because for phase velocities equal to c, the dispersion relation requires the wall radius to be so large that $E_z \ll E_r(r = a)$. In the dielectric liner cases, E_z can
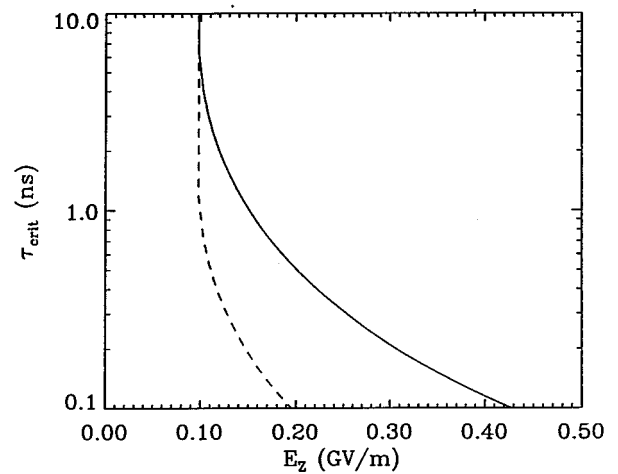

FIG. 9. Plot of critical pulse time τ_{crit} versus the accelerating gradient E_z for a millimeter wave driver, $\lambda = 1$ mm. The inner radius $a = 3$ mm (solid curve), 5 mm (dotted curve), and 10 mm (dashed curve), where $b - a = 5$ mm. In addition, $\varepsilon = 3$, $U_I = 8$ eV, $n_{p0} = 0$, $\nu_m = 10^{15}$ sec^{-1}, and $\nu_0 = 10^{11}$ sec^{-1}.

FIG. 11. Plot of critical pulse time τ_{crit} versus the accelerating gradient E_z for a millimeter wave driver, $\lambda = 1$ mm. The initial electron density n_{p0} is 0 (solid curve) and 1 cm^{-3} (dashed curve). The parameters are $a = 0.2$ mm, $b = 0.283$ mm, $\varepsilon = 10$, $U_I = 8$ eV, $\nu_m = 10^{15}$ sec^{-1}, and $\nu_0 = 10^{11}$ sec^{-1}.
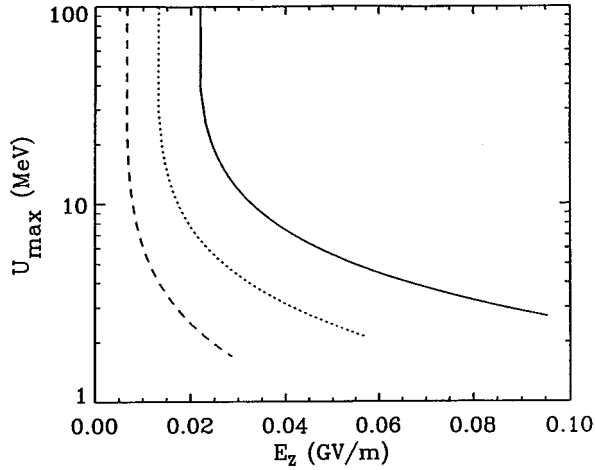
FIG. 12. Plot of maximum electron energy versus accelerating gradient for the parameters in Fig. 9 with $a = 3$ mm (solid curve), 5 mm (dotted curve), and 10 mm (dashed curve).

be the larger field component. Figure 15 is a plot of τ_{crit} versus E_z for a $\lambda = 1$ mm driver with the same three helium gas pressures shown in Fig. 14. The wall radius $a = 26.5$, 14.5, and 8.4 mm for gas pressures P_g of 3, 10, and 30 atm, respectively. The allowable accelerating gradient is a few MV/m. This is due in part to the large a/λ ratio required to have phase velocities equal to c. In addition, the collisional ionization (avalanche) time $1/W$ even at these modest fields is much less than the pulse duration. Figure 16 shows the maximum electron energy U_{max} as a function of the accelerating gradient E_z for the gas-filled ICA using the parameters in Fig. 14, with gas pressures 3, 10, and 30 atm. Comparing Fig. 16 with Figs. 8, 12, and 13 we find that higher acceleration gradients can be obtained in the gas-filled ICA to reach a given maximum energy as compared to the dielectrically lined ICA configuration.
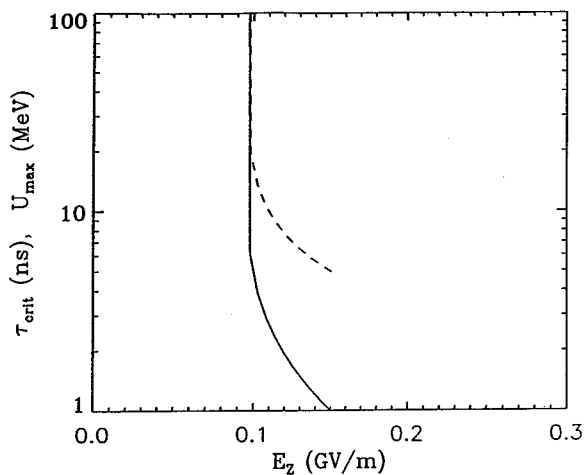
FIG. 14. Plot of critical pulse time τ_{crit} versus the accelerating gradient E_z in a gas- (helium-) filled ICA with laser wavelength $\lambda = 10$ μm. The gas pressures and corresponding wall radii are 3 atm and 265 μm (solid curve), 10 atm and 145 μm (dotted curve), and 30 atm and 84 μm (dashed curve), with $U_I = 24.6$ eV, $\nu_m/P_g = 10^{12}$ sec^{-1}/atm, and $\nu_0/P_g = (2m/M)\nu_m/P_g = 3 \times 10^8$ sec^{-1}/atm.

IX. SUMMARY AND DISCUSSION

The analysis in this paper implies that the combination of ionization and pulse lethargy effects impose severe limitations on the energy gain in inverse Cherenkov accelerators. Two configurations for the ICA have been considered in which the electromagnetic driver (e.g., laser, millimeter, or centimeter wave source) is propagated in a waveguide that is (i) lined with a dielectric material or (ii) filled with a neutral gas. Using a dielectrically lined or gas-filled waveguide, (i) avoids diffraction of the electromagnetic driver beam, (ii) overcomes phase velocity slippage, and (iii) the acceleration

FIG. 13. Plot of critical pulse time τ_{crit} versus the accelerating gradient E_z (solid curve) and U_{max} versus E_z (dashed curve) for $\lambda = 1$ cm and $a = 0.2$ cm. In addition, $b - a = 0.0833$ cm, $\varepsilon = 10$, $U_I = 8$ eV, $n_{p0} = 0$, $\nu_m = 10^{15}$ sec^{-1}, and $\nu_0 = 10^{11}$ sec^{-1}.
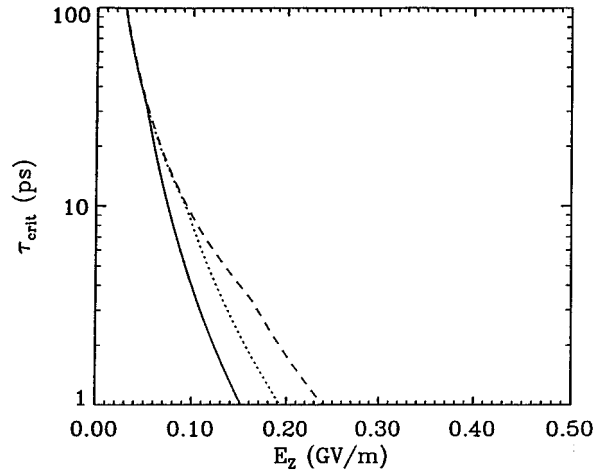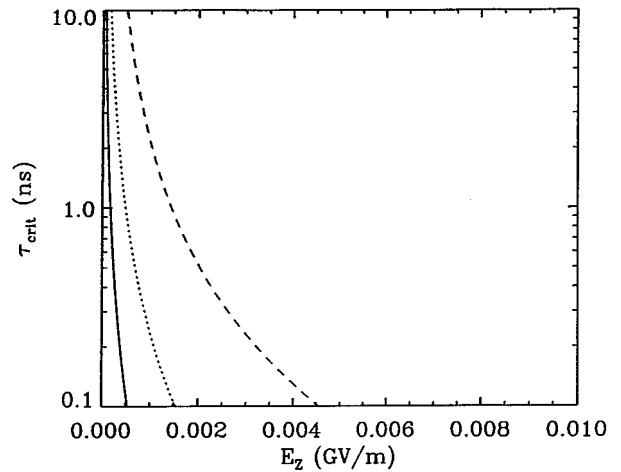
FIG. 15. Plot of critical pulse time τ_{crit} versus the accelerating gradient E_z in a gas- (helium-) filled ICA with laser wavelength $\lambda = 1$ mm. The gas pressures and corresponding wall radii are 3 atm and 26.5 mm (solid curve), 10 atm and 14.5 mm (dotted curve), and 30 atm and 8.4 mm (dashed curve), with $U_I = 24.6$ eV, $\nu_m/P_g = 10^{12}$ sec^{-1}/atm, and $\nu_0/P_g = (2m/M)\nu_m/P_g = 3 \times 10^8$ sec^{-1}/atm.
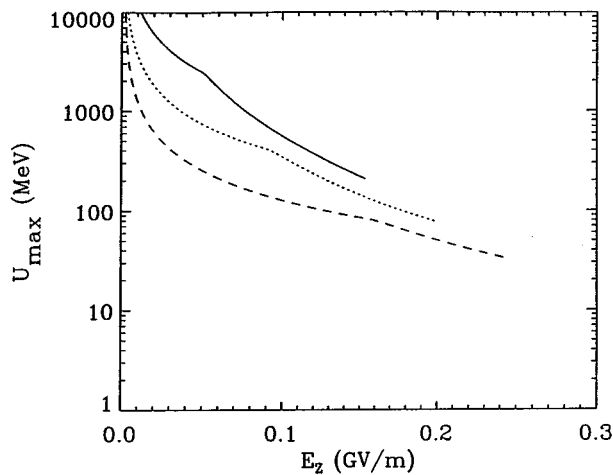
FIG. 16. Plot of maximum electron energy versus accelerating gradient for the parameter in Fig. 14 with $P_g = 3$ atm (solid curve), 10 atm (dotted curve), and 30 atm (dashed curve).

is in vacuum (for the dielectrically lined configuration). In either configuration the electromagnetic driving field has an axial electric field with phase velocity equal to c. The intensity of the driver in the ICA, and therefore the acceleration gradient, is limited by tunneling and collisional ionization effects. Partial volume ionization of the dielectric liner or gas can lead to significant modification of the electromagnetic properties of the waveguide, altering the phase velocity of the accelerating field and causing phase velocity slippage, thus disrupting the acceleration process. Ionization effects therefore impose an upper limit on the driver pulse duration. The driving pulse, however, cannot be arbitrarily short in duration since the pulse, having a group velocity less than c, slips behind the accelerated electrons. This effect is referred to as group velocity slippage or pulse lethargy and places a lower limit on the pulse duration. Limitations on the

driver pulse duration, accelerating gradient, and maximum accelerated electron energy, due to ionization effects and pulse lethargy, have been obtained.

To obtain these limitations a dispersion relation for transverse-magnetic modes of a dielectrically lined and gas-filled optical waveguide has been derived. The TM mode consists of a radial and an axial electric field as well as an azimuthal magnetic field. The axial electric field, which is responsible for acceleration, is peaked on axis, while the radial electric field vanishes on axis. It is shown that when the average plasma density reaches a critical value, due to ionization, the optical properties of the waveguide are modified and the phase velocity of the electromagnetic wave is significantly altered, resulting in phase velocity slippage. The buildup of the plasma within the dielectric material is analyzed using a rate equation which includes tunneling and collisional ionization. We have obtained an expression for the limit on the electromagnetic pulse duration in terms of the accelerating gradient for both the dielectrically lined and gas-filled waveguide ICA configurations. To avoid the effects of ionization, the pulse duration of the electromagnetic driver τ_L in the ICA must be less than a critical pulse duration time τ_{crit} given by Eq. (28). The value of τ_{crit} is a sensitive function of the peak electric field and thus the accelerating gradient. The limitation on the pulse length due to ionization, Eq. (28), together with the limitations imposed by pulse lethargy, Eqs. (43) and (45), present a severe limit on the interaction length and therefore the maximum energy gain, Eq. (46), in the ICA. The maximum accelerated electron energy can be expressed in terms of only the accelerating gradient. Our results indicate that relatively modest accelerating gradients can be achieved in the ICA.

ACKNOWLEDGMENTS

[1] *Advanced Accelerator Concepts*, edited by S. Chattopadhyay, (AIP, New York, in press); *Advanced Accelerator Concepts*, edited by P. Schoessow, AIP Conf. Proc. No. 335 (AIP, New York, 1995); *Advanced Accelerator Concepts*, edited by J. S. Wurtele, AIP Conf. Proc. No. 279 (AIP, New York, 1993).

[2] J. A. Edighoffer and R. H. Pantell, J. Appl. Phys. **50**, 6120 (1979).

[3] E. J. Bochove, G. T. Moore, and M. O. Scully, Phys. Rev. A **46**, 6640 (1992); M. O. Scully and M. S. Zubairv, *ibid.* **44**, 2656 (1991).

[4] P. Sprangle, E. Esarey, and J. Krall, Phys. Plasmas **3**, 2183 (1996).

[5] P. Sprangle, E. Esarey, and J. Krall, Phys. Rev. E **54**, 4211 (1996).

[6] Y. C. Huang, D. Zheng, W. M. Tulloch, and R. L. Byer, Appl. Phys. Lett. **68**, 753 (1996).

[7] Y. C. Huang and R. L. Byer, Appl. Phys. Lett. **69**, 2175 (1996).

[8] P. Sprangle, E. Esarey, J. Krall, and A. Ting, Opt. Commun. **124**, 69 (1996).

[9] E. Esarey, P. Sprangle, and J. Krall, Phys. Rev. E **52**, 5443 (1995).

[10] B. Hafizi, E. Esarey, and P. Sprangle, Phys. Rev. E **55**, 3539 (1997).

[11] B. Hafizi, A. Ting, E. Esarey, P. Sprangle, and J. Krall, Phys. Rev. E (to be published).

[12] J. A. Edighoffer, W. D. Kimura, R. H. Pantell, M. A. Piestrup, and D. Y. Wang, Phys. Rev. A **23**, 1848 (1981).

[13] J. R. Fontana and R. H. Pantell, J. Appl. Phys. **54**, 4285 (1983).

[14] R. D. Romea and W. D. Kimura, Phys. Rev. D **42**, 1807 (1990).

[15] W. D. Kimura, G. H. Kim, R. D. Romea, L. C. Steinhauer, I. V. Pogorelsky, K. P. Kusche, R. C. Fernow, X. Wang, and Y. Liu, Phys. Rev. Lett. **74**, 546 (1995).

[16] J. Rosenzweig, A. Murokh, and C. Pellegrini, Phys. Rev. Lett. **74**, 2467 (1995).

[17] W. Gai, A. D. Kanareykin, A. L. Kustov, and J. Simpson, in *Advanced Accelerator Concepts*, edited by P. Schoessow, AIP Conf. Proc. No. 335 (AIP, New York, 1995), p. 463.

[18] T. B. Zhang, T. C. Marshall, M. L. LaPointe, J. L. Hirshfield, and A. Ron, Phys. Rev. E **54**, 1918 (1996).

[19] B. C. Stuart, M. D. Feit, A. M. Rubenchik, B. W. Shore, and M. D. Perry, Phys. Rev. Lett. **74**, 2248 (1995); B. C. Stuart, M. D. Feit, S. Herman, A. M. Rubenchik, B. W. Shore, and M. D. Perry, Phys. Rev. B **53**, 1749 (1996).

[20] D. Du, X. Liu, G. Korn, J. Squier, and G. Mourou, Appl. Phys. Lett. **64**, 3071 (1994).

[21] Y. P. Raizer, *Gas Discharge Physics* (Springer-Verlag, Berlin, 1991).

[22] Y. B. Zeldovich and Y. P. Raizer, *Physics of Shock Waves and High-Temperature Hydrodynamic Phenomena* (Academic, New York, 1966), Chap. VI.

[23] Y. R. Shen, *The Principles of Nonlinear Optics* (Wiley, New York, 1984).

[24] L. V. Keldysh, Zh. Eksp. Teor. Fiz. **47**, 1945 (1964) [Sov. Phys. JETP **20**, 1307 (1965)].

[25] L. V. Keldysh, Zh. Eksp. Teor. Fiz. **33**, 994 (1957) [Sov. Phys. JETP **6**, 763 (1958)].

[26] B. Hafizi, P. Sprangle, and A. Ting, in *Advanced Accelerator Concepts*, edited by P. Schoessow, AIP Conf. Proc. No. 335 (AIP, New York, 1995), p. 480.